Organic Electronics 24 (2015) 176–181

Contents lists available at ScienceDirect

Organic Electronics

journal homepage: www.elsevier.com/locate/orgel

Low dark current inverted organic photodetectors employing MoO_x:Al cathode interlayer

Dong-Seok Leem [a], Kwang-Hee Lee [a], Young-Nam Kwon [b], Dong-Jin Yun [b], Kyung-Bae Park [a], Seon-Jeong Lim [a], Kyu-Sik Kim [a], Yong Wan Jin [a,*], Sangyoon Lee [a]

[a] Organic Materials Lab., Samsung Advanced Institute of Technology (SAIT), Samsung Electronics Co., 130 Samsung-ro, Suwon-si, Gyeonggi-do 443-803, Republic of Korea
[b] Analytical Science Group, Samsung Advanced Institute of Technology (SAIT), Samsung Electronics Co., 130 Samsung-ro, Suwon-si, Gyeonggi-do 443-803, Republic of Korea

ARTICLE INFO

Article history:
Received 27 February 2015
Received in revised form 8 May 2015
Accepted 29 May 2015
Available online 30 May 2015

Keywords:
Organic photodetectors
Inverted structure
Cathode interlayer
Low dark current

ABSTRACT

We report low dark current small molecule organic photodetectors (OPDs) with an inverted geometry for image sensor applications. Adopting a very thin MoO_x:Al cathode interlayer (CIL) in the inverted OPD with a reflective top electrode results in a remarkably low dark current density (J_d) of 5.6 nA/cm^2 at reverse bias of 3 V, while maintaining high external quantum efficiency (EQE) of 56.1% at visible wavelengths. The effectiveness of the CIL on the diode performance has been further identified by application to inverted OPDs with a semi-transparent top electrode, leading to a significantly low J_d of 0.25 nA/cm^2, moderately high $EQE_{540\ nm}$ of 25.8%, and subsequently high detectivity of 8.95×10^{12} Jones at reverse bias of 3 V. Possible origins of reduced dark currents in the OPD by using the MoO_x:Al CIL are further described in terms of the change of interfacial energy barrier and surface morphology.

1. Introduction

Organic photodetectors (OPDs) have recently been acknowledged as one of the prospective candidates for image sensor applications [1–8]. For instance, adopting OPDs as light sensitive components on conventional thin film transistors (TFT) [2,3] or complementary metal oxide semiconductor (CMOS) circuits [4,5], has initiated the proof-of-concept of high sensitivity hybrid image sensors by accomplishing a pixel filling factor close to 100% [2,4,5]. To truly realize highly sensitive organic–inorganic hybrid imagers, however, achieving high performance OPDs is crucial. Among diode characteristics, suppressing dark currents under reverse bias while maintaining high external quantum efficiency (EQE) is of great importance due to the major influence on the subsequent figures of merit for OPDs, i.e., specific detectivity (D^*) and linearity [6,7]. Considerable efforts have been devoted to reduce the dark current of OPDs mainly by means of the insertion of additional interfacial layers and the thickness modulation of the light absorbing layer, leading to low dark current density (J_d) in the range of 1–10 nA/cm^2 and the consequently high D^* over 10^{12} Jones [6–11].

While most investigations have been carried out based on the normal OPD structure, rather less attention [12–14] has been given to the inverted geometry for OPDs, in which the layer sequence is reversed and electrons are collected via the bottom electrode of the OPD, facilitating its integration with a low work function metallization in TFT or CMOS circuits for hybrid imagers [4,12,13]. Since a wide range of inverted structures have been already applied to organic photovoltaics (OPVs) [15–17], it seems that deriving relevant device geometries (i.e., interfacial buffer layers) from inverted OPVs enables easier approach to make high quality inverted OPDs. However, OPVs typically focus on the improvement of short-circuit current and fill factor without any external reverse bias, whereas OPDs highlight the achievement of low J_d, high photocurrent under reverse bias condition, and even fast photoresponse speed for the imaging application [6,7,14]. This suggests that dominant factors to determine figures of merit for the OPD and OPV are fundamentally different [14], requiring further insights into the realization of high performance OPDs with the inverted geometry. Very recently, Saracco et al. [14] has examined reduction of J_d in solution-processed inverted OPDs by adopting a well-known interfacial layer of ethoxylated polyethylenimine (PEIE), demonstrating a significantly low J_d of 2 nA/cm^2 at reverse bias of 2 V and moderate EQE of 30% at visible wavelengths. In order to further systematically investigate the impact of the interfacial buffer layer on the performance of inverted OPDs, in this study, we have introduced a unique cathode interlayer (CIL) of the MoO_x:Al by co-evaporation [16]. The interlayer has previously been shown to improve the efficiency of inverted OPVs, acting as an efficient electron extraction layer [16] and here we find that it

* Corresponding author.
E-mail address: ywjin@samsung.com (Y.W. Jin).

http://dx.doi.org/10.1016/j.orgel.2015.05.044
1566-1199/

also has a beneficial influence on the reduction of reverse J_d in inverted OPDs, while maintaining high EQE and subsequently high D^* over 10^{12} Jones.

2. Experimental

Fig. 1(a) exhibits the inverted device structure used in this study comprising an ITO-coated glass substrate, a 5 nm MoO_x:Al interlayer with a 1:1 mixing ratio, a 70 nm bulk heterojunction (BHJ) of *N*,*N*-dimethylquinacridone (DMQA) and dicyanovinyl-substituted terthiophene derivative (DCV3T) with a blend ratio of 1:1 [11], a 30 nm MoO_x hole extraction layer, and an 80 nm thick Al electrode (hereinafter referred to as a reflective inverted OPD). The control device was fabricated with the interlayer omitted. All films were thermally evaporated (<10^{-7} Torr) and the device was finally encapsulated with glass. The pixel size, defined by the overlap of the two electrodes, was 0.04 cm^2. The possible energy level diagrams of the OPD structure are depicted in Fig. 1(b). The MoO_x:Al interlayer was also applied to semi-transparent inverted OPDs with a thicker BHJ (110 nm), in which the layer structure is identical except the replacement of the reflective top Al electrode by a thin Ag electrode (11 nm) and an additional anti-reflection coating layer (30 nm) of triphenylamine derivative [11] (see the inset of Fig. 6(a) for details). For comparison, reference devices with PEIE interlayers were additionally prepared by spin-coating the diluted solution (0.4 wt% in 2-methoxyethanol) onto the ITO substrate at spin speeds of 2000–5000 rpm for 30 s followed by annealing at 100 °C for 10 min in nitrogen ambient [14]. A pristine DCV3T layer (10 nm) was also introduced as a hole blocking layer (HBL) between the interlayer and the BHJ for further decrease in device dark currents.

The influence of the MoO_x:Al CIL on the electrical property of the ITO electrode was monitored by the ultraviolet photoemission spectroscopy (UPS) measurement (Versaprobe PHI 5000) using He I (21.2 eV) excitation source. The secondary electron cut-off revealed a reduction in the ITO work function by ca. 0.40 eV from 4.71 eV to 4.31 eV when a 5 nm layer of MoO_x:Al was deposited on ITO (not shown). The AFM (Veeco, Dimension V) was used to characterize the film morphology. The current density–voltage (*J*–*V*) characteristics of diodes were measured by a Keithley 4200 parameter analyzer. The photocurrent characteristics were evaluated under illumination by a green laser diode (λ = 553 nm) with different light intensities in the range of 0.1–10 mW/cm^2. The EQE was measured using a setup illuminated by monochromatic light generated by an ozone-free Xenon lamp with a chopper frequency of 30 Hz. The monochromatic light intensity was calibrated using a silicon photodiode (Hamamatsu, S1337). The corresponding photoresponsivity (*R*) (A/W) defined as the ratio of generated photocurrent (A) to incident light power (W) was converted from the EQE using $R = EQE/h\nu$, where $h\nu$ is the energy of the incident photon in electron volts (eV) [6,11]. The frequency response was evaluated using the measurement setup consisting of a 500-MHz bandwidth oscilloscope (LeCroy Wavejet 352A), a function generatior (LeCroy WaveStation 2012), and a green laser diode (λ = 553 nm, 10 mW/cm^2).

3. Results and discussion

Typical *J*–*V* characteristics of reflective inverted OPDs measured in the dark are shown in Fig. 2(a). The interlayer-free device clearly exhibited high leakage currents with increasing the reverse bias. For instance, the device showed high J_d of 5.13×10^{-7} ($\pm 2.53 \times 10^{-7}$) A/cm^2 at reverse bias of 3 V and an inferior injection current as low as 1.71×10^{-6} A/cm^2 at forward bias of −3 V. We note that reverse bias of 3 V was typically selected as a reference voltage for realizing efficient OPDs with a low operational voltage and the consequent application to image sensors with low power consumption. Inserting a 5 nm CIL of MoO_x:Al in the OPD, by contrast, led to a remarkable decrease in the reverse dark current, showing a significantly low J_d of 5.57×10^{-9} ($\pm 2.47 \times 10^{-9}$) A/cm^2 at 3 V, which is almost two orders of magnitude lower than the J_d value of the interlayer-free OPD. It is also noted that the forward injection current of the CIL device markedly increased, resulting in a high rectification ratio of 3.1×10^5 at ±3 V. These results imply that the MoO_x:Al CIL can indeed act both as an electron injection layer at forward bias condition and a HBL at reverse bias. Note that since we have clearly observed the change of dark *J*–*V* characteristics by solely modifying the surface of the ITO cathode under a fixed hole buffer layer (MoO_x), reverse bias-induced hole injection currents from the ITO cathode are considered as the dominant route to the J_d of OPDs (see Fig. 1(b)).

The photocurrent densities (J_{ph}) of corresponding OPDs measured at reverse bias of 3 V under light illumination at 553 nm are plotted in Fig. 2(b), which exhibit the linear increase of J_{ph} of OPDs with increasing the light intensity. The OPD with the MoO_x:Al CIL showed higher J_{ph} compared to the interlayer-free device, indicating that the MoO_x:Al layer efficiently enhanced the extraction of photogenerated charges caused by the reduction in the energetic barrier between the effective Fermi level of the ITO cathode and the LUMO level of the acceptor (DCV3T) in the BHJ blend [16]. A figure of merit for determining the linearity of OPDs, i.e., the linear dynamic range (LDR) [6,11] was calculated

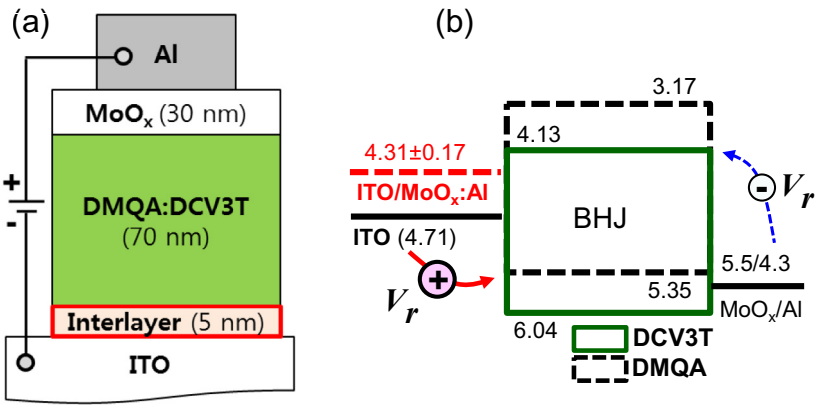

Fig. 1. (a) Schematic representation of the inverted OPD with a reflective top electrode. (b) The corresponding energy level diagram of the OPD. Note that V_r indicates an applied voltage under reverse bias.